Extracellular proton modulation of the cardiac voltage-gated sodium channel, $Na_V1.5$

Supporting Material

Jones, D.K.[†], C.H. Peters[†], S.A. Tolhurst[†], T.W. Claydon[†], P.C. Ruben[†]*

* To whom correspondence should be addressed:

Peter C. Ruben
Department of Biomedical Physiology and Kinesiology
Simon Fraser University
8888 University Drive
Burnaby, BC V5A 1S6
pruben@sfu.ca

[†] Department of Biomedical Physiology and Kinesiology
Simon Fraser University
8888 University Drive
Burnaby, BC V5A 1S6
Canada

SUPPLEMENTARY MATERIAL

Activation, Fast Inactivation, and Slow Inactivation Analysis

Conductance curves were computed from current/voltage relationships using the equation:

$$\text{Equation S1:} \quad G = I_{max}/(V_m - E_{rev})$$

where, G is conductance, I_{max} represents the peak test pulse current, V_m is the test pulse voltage, and E_{rev} is the measured reversal potential. Values were plotted as a function of test potential and then fitted with the Boltzmann equation:

$$\text{Equation S2:} \quad f(x) = 1/(1+\exp(-ze_0(V_m - V_{1/2})kT))$$

where, z is the apparent valence, e_0 is the elementary charge, $V_{1/2}$ is the midpoint, T is the recording temperature in °K, and k is the Boltzmann constant. Steady-state fast inactivation and steady-state slow inactivation data were fitted with a modified Boltzmann equation:

$$\text{Equation S3:} \quad f(x) = (I_1 - I_2)/(1 + \exp(-ze_0(V_m - V_{1/2})kT)) + I_2$$

where, I_1-I_2 are the maximum and minimum values of the fit, respectively. All other values are identical to Equation S2. The time constants of the recovery and onset of fast inactivation and the recovery (pH 6.0 only) and onset of slow inactivation were calculated from the single exponential equation:

$$\text{Equation S4:} \quad f(x) = Y_o + A\exp(-x/\tau)$$

where, Y_0 is the asymptote of the fit, A is the relative component of the exponent, τ is the time constant, and x is time. The time constants of fast inactivation onset and recovery were plotted as a function of prepulse and interpulse voltage, respectively, and fitted with the Eyring model:

$$\text{Equation S5:} \quad f(x) = 1/[(\tau_M \exp(-wb(V - V_P)/T)) + (\tau_M \exp(w(1-b)(V - V_P)/T))]$$

where, τ_M is the inverse of the maximum time constant, w is the reaction velocity, b is the barrier distance, V is the voltage, V_P is the voltage at the peak of the fit, and T is the temperature. Slow inactivation recovery (pH 7.4 only) and use-dependent inaction data were fitted with the double exponential equation:

$$\text{Equation S6:} \quad f(x) = Y_o + A_1\exp(-x/\tau_1) + A_2\exp(-x/\tau_2)$$

where, Y_0 is the asymptote of the fit, A_1 is the relative component of the first exponent, τ_1 is the slow time constant, A_2 is the relative component of the second exponent, τ_2 is the fast time constant and x is time. Goodness of fit for slow inactivation recovery data was based on reduced χ^2 analyses.

Modeling Parameters

The original ten Tusscher model (1) was programmed into Python code using the modules NumPy© (Enthought Inc., Austin, TX, USA), matplotlib© (John Hunter). The code was then updated to include their new calcium current and slow delayed potassium current equations (2, 3). A late persistent sodium current was added following the formulas of Hund and Rudy (4). The maximal sodium conductance value was replaced with the Luo-Rudy dynamic model value to better reflect our experimental data (5). The slow delayed rectifier potassium conductance (G_{Kr}) was changed to incorporate the role of internal calcium concentrations on G_{Ks} (6). The late sodium maximal conductance value was changed to reflect the data collected by (7). These data show the differing persistent sodium current in the different types of cardiac myocytes. We collected slow inactivation recovery time constants at -150 mV and -130 mV and time constants of slow inactivation onset at 0 mV and 20 mV. To incorporate a range of time constants that would coincide with the voltages of a ventricular action potential, as was done for the kinetics of fast inactivation, the slow inactivation time constants that we collected were normalized to those collected by Richmond et al. (1998). This allowed us to generate a range of time constants applicable to the spectrum of voltages in a ventricular action potential (8). The new time constants were then fitted with two exponential equations and incorporated into the model (8). Finally, our (1) steady-state conductance and inactivation curves, (2) fast and slow inactivation time constants of both recovery and onset, and (3) normalized late sodium currents were incorporated into the model to reflect the different sodium current properties at pH 7.4 versus pH 6.0. The model was run for epicardial, mid-myocardial, and endocardial ventricular cardiomyocytes at 1 Hz (Fig. 6). Time constants for onset and recovery of fast inactivation and slow inactivation were also adjusted to be consistent with our experimentally-derived measurements of these parameters. Tables S1, S2, and S3 outline the specific values of the parameters used in the model.

Table S1: Modeling parameters of steady-state activation and fast inactivation

	V½		z		Proton Block Scaling Factor @ pH 6.0
	pH 7.4	pH 6.0	pH 7.4	pH 6.0	
Activation	-35.49	-35.49	3.35	3.35	0.62
Fast inactivation	-77.16	-73.23	-4.75	-4.46	

Table S2: Modeling parameters of steady-state slow inactivation

V½		z		Maximal probability of SI pH 7.4	Maximal probability of SI, pH 6.0
pH 7.4	pH 6.0	pH 7.4	pH 6.0		
-82.66	-83.09	-3.63	-3.13	0.52	0.53

Steady-state values of the fits from Table S1 and Table S2 were derived using:
Eq. S3: $f(x) = 1/(1+\exp(-ze_0(V_m-V_{1/2})kT))$,
Eq. S4: $f(x) = (I_1-I_2)/(1 + \exp(-ze_0(V_m-V_{1/2})kT)) + I_2$

Table S3: Maximal conductance of late sodium current

	Epicardial	Endocardial	Mid-Myocardial
pH 7.4	0.0565	0.0650	0.1910
pH 6.0	0.0853	0.0982	0.2884

Supplementary Figures
Figure S1

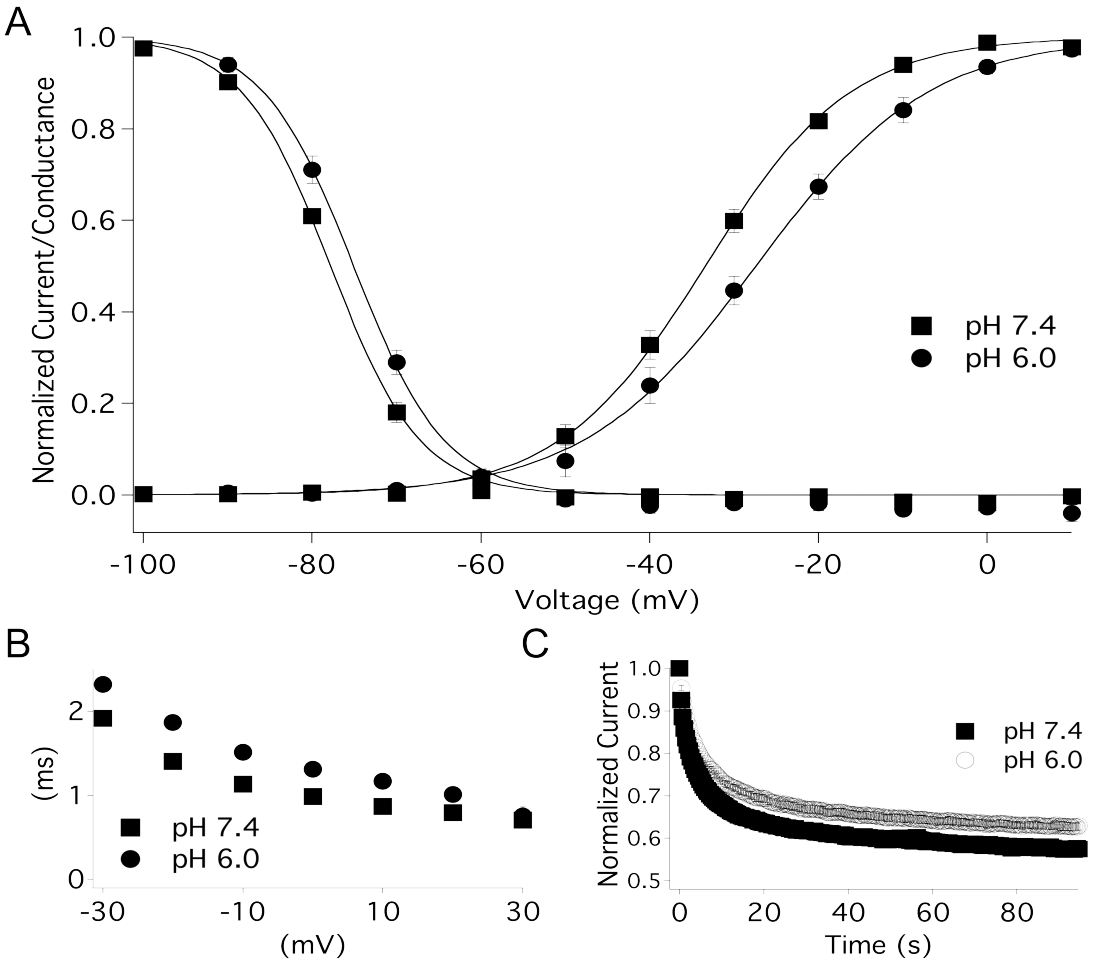

Figure S1.
pH modulation of $Na_V1.5$–β_1 subunit. (*A*) Normalized conductance and steady-state fast inactivation curves recorded from $Na_V1.5$ expressed without the β_1 subunit at pH 7.4 (*squares*) and pH 6.0 (*circles*). (B) Open-state fast inactivation kinetics of $Na_V1.5$ recorded at pH 7.4 (*squares*) and pH 6.0 (*circles*). Time constants are plotted as a function of test potential. (*C*) Use-dependent inactivation of $Na_V1.5$ recorded at pH 7.4 (*squares*) and pH 6.0 (*circles*). All effects were slightly smaller than, but not statistically different from, those observed in $Na_V1.5+\beta_1$.

Figure S2

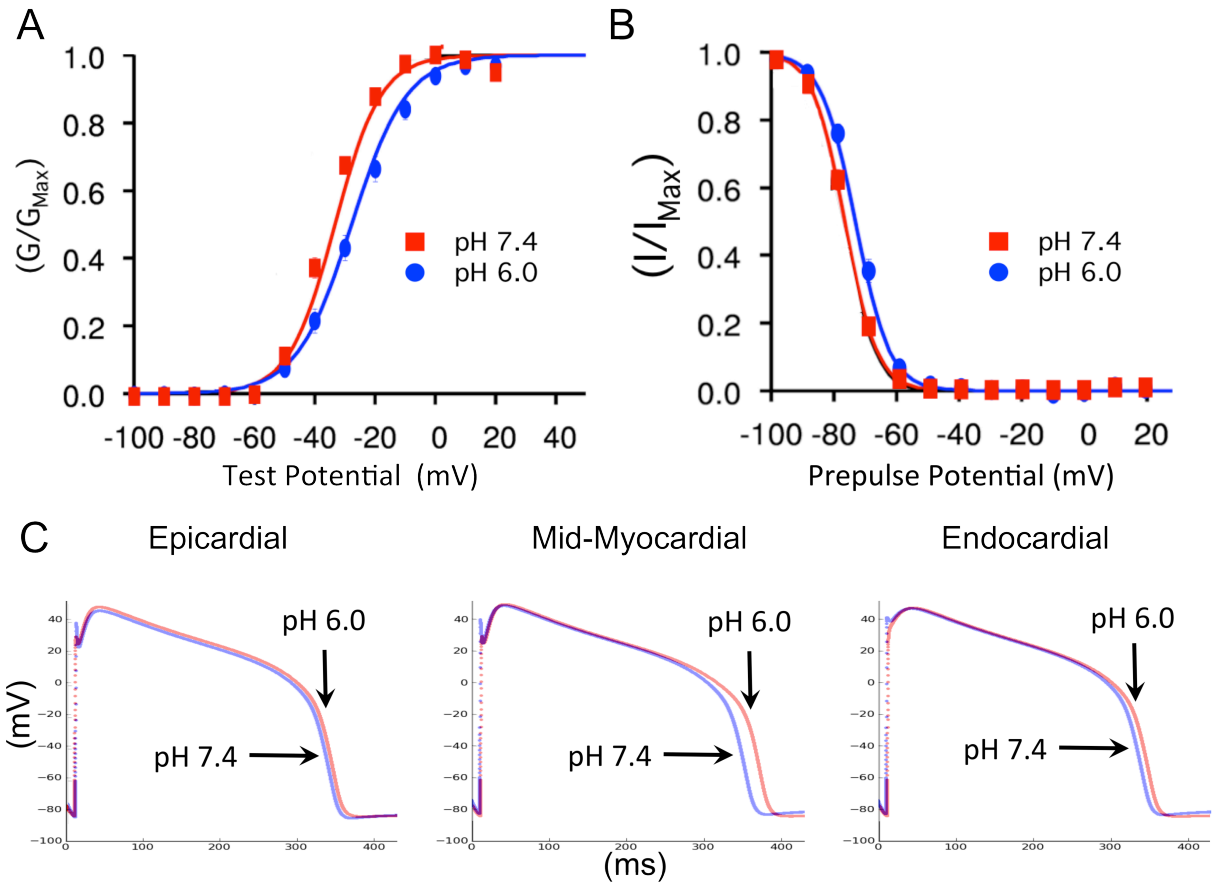

Figure S2. Modeling recapitulates experimental data. (*A* and *B*) Conductance and steady-state fast inactivation curves in $Na_V1.5+\beta_1$ recorded at pH 7.4 (*squares*) and pH 6.0 (*circles*). Fit lines represent modeling data at each respective pH. (*C*) Modeled epicardial, mid-myocardial, and epicardial human ventricular action potentials incorporating $Na_V1.5+\beta_1$ data recorded at pH 7.4 (*blue*) and pH 6.0 (*red*). pH 6.0 data preferentially prolonged mid-myocardial action potentials over epicardial and endocardial action potentials.

References

1. ten Tusscher, K. H., D. Noble, P. J. Noble, and A. V. Panfilov. 2004. A model for human ventricular tissue. Am J Physiol Heart Circ Physiol 286:H1573-1589.
2. ten Tusscher, K. H., and A. V. Panfilov. 2006. Cell model for efficient simulation of wave propagation in human ventricular tissue under normal and pathological conditions. Phys Med Biol 51:6141-6156.
3. ten Tusscher, K. H., and A. V. Panfilov. 2006. Alternans and spiral breakup in a human ventricular tissue model. Am J Physiol Heart Circ Physiol 291:H1088-1100.
4. Hund, T. J., and Y. Rudy. 2004. Rate dependence and regulation of action potential and calcium transient in a canine cardiac ventricular cell model. Circulation 110:3168-3174.
5. Luo, C. H., and Y. Rudy. 1994. A dynamic model of the cardiac ventricular action potential. I. Simulations of ionic currents and concentration changes. Circ Res 74:1071-1096.
6. Terrenoire, C., C. E. Clancy, J. W. Cormier, K. J. Sampson, and R. S. Kass. 2005. Autonomic control of cardiac action potentials: role of potassium channel kinetics in response to sympathetic stimulation. Circ Res 96:e25-34.
7. Zygmunt, A. C., G. T. Eddlestone, G. P. Thomas, V. V. Nesterenko, and C. Antzelevitch. 2001. Larger late sodium conductance in M cells contributes to electrical heterogeneity in canine ventricle. Am J Physiol Heart Circ Physiol 281:H689-697.
8. Richmond, J. E., D. E. Featherstone, H. A. Hartmann, and P. C. Ruben. 1998. Slow inactivation in human cardiac sodium channels. Biophys J 74:2945-2952.